Domain Wall Tilting in the Presence of the Dzyaloshinskii-Moriya Interaction in Out-of-Plane Magnetized Magnetic Nanotracks

O. Boulle,[1,*] S. Rohart,[2] L. D. Buda-Prejbeanu,[1] E. Jué,[1] I. M. Miron,[1] S. Pizzini,[3] J. Vogel,[3] G. Gaudin,[1] and A. Thiaville[2]

[1]*SPINTEC, CEA/CNRS/UJF/INPG, INAC, 38054 Grenoble Cedex 9, France*

[2]*Laboratoire Physique des Solides, Université Paris-Sud, CNRS UMR 8502, 91405 Orsay, France*

[3]*Institut Néel, CNRS and UJF, 25 avenue des Martyrs, B.P. 166, 38042 Grenoble Cedex 9, France*

(Received 4 April 2013; revised manuscript received 1 August 2013; published 20 November 2013)

We show that the Dzyaloshinskii-Moriya interaction (DMI) can lead to a tilting of the domain wall (DW) surface in perpendicularly magnetized magnetic nanotracks when DW dynamics are driven by an easy axis magnetic field or a spin polarized current. The DW tilting affects the DW dynamics for large DMI, and the tilting relaxation time can be very large as it scales with the square of the track width. The results are well explained by an extended collective coordinate model where DMI and DW tilting are included. We propose a simple way to estimate the DMI in magnetic multilayers by measuring the dependence of the DW tilt angle on a transverse static magnetic field. These results shed light on the current induced DW tilting observed recently in Co/Ni multilayers with structural inversion asymmetry.

DOI: 10.1103/PhysRevLett.111.217203 PACS numbers: 75.70.Tj, 75.60.Ch, 75.78.−n, 85.75.−d

The effect of structural inversion asymmetry (SIA) on the magnetic and electronic transport properties at interfaces of low dimensional magnetic films is currently attracting growing attention. In the presence of spin-orbit coupling, SIA leads to an additional term in the exchange interaction, namely the Dzyaloshinskii-Moriya interaction (DMI) [1,2], which tends to make the magnetization rotate around a local characteristic vector D. This can destabilize the uniformly magnetized states leading to novel chiral magnetic orders, such as spin spirals [3]. Novel out-of-equilibrium transport phenomena have also been demonstrated, such as current induced spin-orbit torques induced by the Rashba spin-orbit coupling and/or the spin Hall effect, leading to current induced magnetization reversal [4–6]. A recent striking example of the impact of SIA in ultrathin magnetic films is the current induced domain wall motion (CIDM) in perpendicularly magnetized nanotracks. This was first outlined by Miron *et al.* who reported very efficient CIDM in asymmetric Pt/Co (0.6 nm)/Al oxide (AlOx) multilayers, whereas symmetric Pt/Co/Pt multilayers showed no effects [7,8]. The high perpendicular anisotropy in this material leads to narrow domain walls (DWs) (∼5 nm), so that in typical experiments, the nanotrack width (∼100 nm) is much larger than the DW width. Thus, it is expected that the magnetization rotates parallel to the DW surface (Bloch DWs) to minimize the magnetostatic energy. Whereas these experiments were first interpreted in terms of a high nonadiabatic torque induced by the Rashba spin-orbit coupling, it was recently proposed that the high efficiency arises from two key features resulting from SIA and the high spin-orbit coupling in this material [9]: First, the change of the DW equilibrium structure from Bloch to Néel induced by the DMI. This leads to chiral DWs where the DW magnetization rotates perpendicular to the DW surface with a unique sense of rotation [10,11]. Second, a large Slonczewski-like spin-orbit torque (SOT) which is maximal in the Néel configuration [4,12,13]. Recent CIDM experimental results in Pt/Co/Ni [14] and Pt/CoFe/MgO multilayers [15] with SIA seem to support this scheme.

In this Letter, we show that SIA not only affects the DW dynamics through a change of the internal DW structure but also through a modification of its geometrical shape. In perpendicular magnetized nanotracks, the DW surface is expected to be perpendicular to the nanotrack axis to minimize the DW energy. However, in the presence of DMI, when driving the DW dynamics, micromagnetics reveals that a large DMI can lead to a sizable tilting of the DW surface which can strongly affect the DW dynamics. This DW tilting is a dynamical effect which occurs whatever the driving mechanism, e.g., an external magnetic field or a spin polarized current, and thus, is intrinsically different from the previously reported current induced DW tilting [16–19]. The results are well explained using an analytical model based on a Lagrangian approach where the DMI and the DW tilting are included. We also show that the DW tilting can be controlled using a static transverse magnetic field, providing a simple way to measure the DMI. Our results shed light on the unexplained current induced DW tilting observed in Co/Ni asymmetric multilayer nanotracks [20] and are in agreement with the presence of DMI in these samples [14].

We consider a magnetic ultrathin film grown on a substrate with a capping layer in a different material so that the inversion symmetry is broken along the vertical axis (z). The magnetization is supposed oriented out-of-plane with a strong perpendicular anisotropy. In addition to the standard micromagnetic energy density which includes the exchange, anisotropy, Zeeman and demagnetizing energy, we add the following DMI that reads in a continuous

form [9] $E_{\mathrm{DM}} = D[m_z(\partial m_x/\partial x) - m_x(\partial m_z/\partial x) + (x \rightarrow y)]$. This form corresponds to a sample isotropic in the plane, where the Dzyaloshinskii vector for any in-plane direction $\mathbf{u}$ is $D\mathbf{z} \times \mathbf{u}$ with D a uniform constant, originating from the symmetry breaking at the z surface. Micromagnetic simulations are based on the Landau-Lifschitz-Gilbert equation

$$\frac{\partial \mathbf{m}}{\partial t} = -\frac{\gamma_0}{\mu_0 M_s}\frac{\delta E}{\delta \mathbf{m}} \times \mathbf{m} + \alpha \mathbf{m} \times \frac{\partial \mathbf{m}}{\partial t} - \gamma_0 H_{\mathrm{SO}} J \mathbf{m} \times (\mathbf{m} \times \mathbf{u}_y), \quad (1)$$

where $\gamma_0 = \mu_0|\gamma|$ with γ the gyromagnetic ratio, E the energy density and M_s the saturation magnetization. We assume that the injection of a current density J in the nanotrack leads to a Slonczewski-like torque $-\gamma_0 H_{\mathrm{SO}} J \mathbf{m} \times (\mathbf{m} \times \mathbf{u}_y)$ [4,6,21]. To simplify, we do not consider the effect of the adiabatic and nonadiabatic spin transfer torque nor the fieldlike part of the SOT [19,21,22]. In the following, we consider sufficiently large values of D ($D > 0.12$ mJ/m^2 for our simulation parameters) so that the Néel configuration is stable at equilibrium [9]. 2D micromagnetic simulations are performed using modified homemade micromagnetic solvers [9,23,24]. The following parameters have been used [8]: exchange parameter $A = 10^{-11}$ J/m, saturation magnetization $M_s = 1.09 \times 10^6$ A/m, uniaxial anisotropy constant $K = 1.25 \times 10^6$ J/m^3, Gilbert damping parameter $\alpha = 0.5$, thickness of magnetic layer $t_m = 0.6$ nm.

The DW tilting induced by the DMI can simply be introduced by considering the effect of a static in-plane magnetic field H_y transverse to the magnetic track [Fig 1(b)]. In the presence of H_y, the Zeeman interaction leads to a rotation of the DW magnetization away from the Néel configuration. To recover the Néel configuration energetically favored by the DMI, the DW surface tilts by an angle χ at the cost of a higher DW energy due to the larger DW surface. Figure 1(b) shows the resulting DW tilting for $\mu_0 H_y = 100$ mT and a large value $D = 2$ mJ/m^2. The tilt angle as a function of H_y and D is plotted on Figs. 1(c) and 1(d). As expected, the DW tilting increases with H_y and, for a fixed H_y, increases with D. The tilt angle can be roughly estimated from energetic considerations assuming that the DW always stays in a Néel configuration with an energy per unit surface σ_0 (large D limit). On the one hand, for a DW tilted by an angle χ, the DW surface and, thus, the total energy are increased by a factor $1/\cos\chi$; on the other hand, the Zeeman energy per unit surface scales as $\sigma_Z \sin\chi$ with $\sigma_Z = -\pi\mu_0 H_y M_s \Delta$ (Δ is the DW width). This leads to a total DW energy $E_{\mathrm{DW}} \approx w t_m(\sigma_0 - \sigma_Z \sin\chi)/\cos\chi$, where w is the track width. The minimization of this energy leads to $\sin\chi = \sigma_Z/\sigma_0$. Importantly, the slope of the DW tilting as a function of H_y on Fig. 1(c) depends directly on the value of D. This provides a direct way to measure D, from the dependence of the DW equilibrium tilt angle on H_y.

In the presence of DMI, a tilting of the DW surface can also be induced dynamically by applying an easy axis external magnetic field H_z. The magnetization distribution in the track for different magnetic fields and

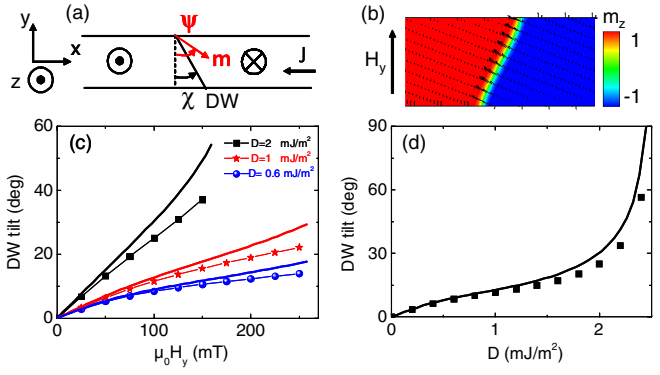

FIG. 1 (color online). (a) Schematic of the tilted DW. (b) Micromagnetic configuration of a 100-nm-wide track with $D = 2$ mJ/m^2 and a transverse magnetic field $\mu_0 H_y = 100$ mT. (c) DW tilt angle as a function of $\mu_0 H_y$ for several values of D and (d) as a function of D for $\mu_0 H_y = 100$ mT. Dots are the results of micromagnetic simulations, whereas the continuous lines are the results of the collective coordinates model described later.

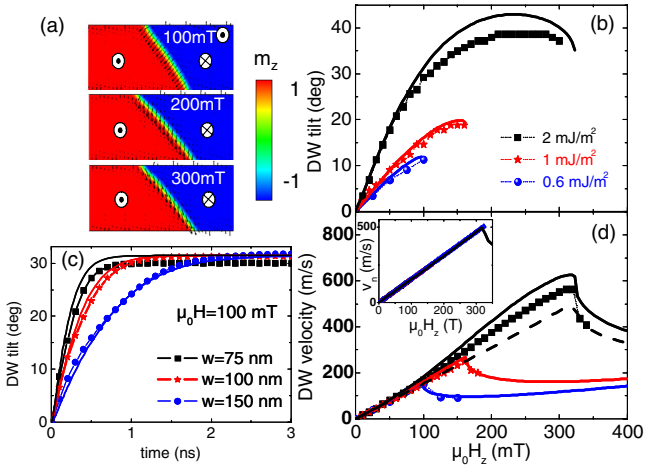

FIG. 2 (color online). Dynamics of the DW driven by an external magnetic field H_z for a 100-nm-wide nanotrack. (a) Magnetization pattern of the DW for different values of H_z with $D = 2$ mJ/m^2. Tilt angle (b) and velocity (d) of the DW as a function of H_z for different values of D. The inset in (d) shows the DW velocity v_n in the direction perpendicular to the DW surface ($v_n = v\cos\chi$). (c) Time dependence of the tilt angle for $\mu_0 H_z = 100$ mT applied at $t = 0$ and different track widths w for $D = 2$ mJ/m^2. In (b)–(d), the results of the micromagnetic simulation (resp. CCM) are plotted in colored dots (resp. continuous lines). The dashed (resp. continuous) black line in (d) (resp. (d), inset) corresponds to the prediction of the standard (q, ψ) model for $D = 2$ mJ/m^2.

$D = 2$ mJ/m^2 [Fig. 2(a)] reveals that the DW tilts significantly in the steady state regime when driven by H_z. As shown on Fig. 2(b), the steady-state tilt angle rapidly increases with H_z and D, although a saturation is observed for large H_z. Figure 2(d) shows the DW velocity v along the track direction as a function of H_z for different values of D. As expected, the DMI leads to an increase of the Walker field [9]. For large values of H_z, the DW velocity significantly deviates from the expected linearity as D increases. This deviation is the result of the DW tilting: the propagation of the tilted DW at a velocity v_n normal to its surface leads to a velocity $v = v_n/\cos\chi$ along the track direction. When considering v_n instead of v [Fig. 2(d), inset], a linear scaling is obtained and the velocity in the steady state regime does not depend on D. Thus, the DW tilting does not affect the DW velocity perpendicular to the DW surface. The time dependence of the DW tilt angle is shown on Fig. 2(c) for several values of the track width w when applying $\mu_0 H_z = 100$ mT at $t = 0$ [25].

To describe the dynamics of tilted DWs induced by the DMI, we consider an extended collective coordinate model (CCM) [26] where the DW is described by three variables: its position in the track q, the DW magnetization angle ψ, and the tilt angle of the DW surface χ [cf. Fig. 1(a)]. The DW profile is described by the following ansatz for the azimuthal θ and polar angle φ [with the definition $\mathbf{m} = (\sin\theta\cos\varphi, \sin\theta\sin\varphi, \cos\theta)$]: $\varphi(x, y, t) = \psi(t) - \pi/2$ and $\theta = 2\arctan\{\exp[(x\cos\chi + y\sin\chi - q\cos\chi)/\Delta]\}$ [$\Delta = \sqrt{A/(K - \mu_0 M_s^2/2)}$ is the DW width]. The effect of the DMI on the DW profile and DW dynamics is taken into account by an additional term in the DW energy (see below) [9]. To derive the dynamical equations, a Lagrangian approach is considered [27–29]. The Landau-Lifschitz-Gilbert equation can be derived by writing the Lagrange-Rayleigh equations for the Lagrangian $L = E + (M_s/\gamma)\varphi\dot{\theta}\sin\theta$ with E the micromagnetic energy density. The effects of the damping and SOT are included by considering the dissipative function $F = \alpha M_s/(2\gamma)[d\mathbf{m}/dt - (\gamma_0/\alpha)H_{SO}J\mathbf{m}\times\mathbf{u}_y]^2$.

The Lagrange-Rayleigh equations then lead to the following CCM equations:

$$\dot{\psi} + \frac{\alpha\cos\chi}{\Delta}\dot{q} = \gamma_0 H_z + \frac{\pi}{2}\gamma_0 H_{SO} J\sin\psi, \tag{2}$$

$$\frac{\dot{q}\cos\chi}{\Delta} - \alpha\dot{\psi} = \frac{\gamma_0 H_k}{2}\sin 2(\psi - \chi) + \frac{\pi D\gamma_0}{2\mu_0 M_s\Delta}\cos(\psi - \chi) - \frac{\pi}{2}\gamma_0 H_y\sin\psi, \tag{3}$$

$$\dot{\chi}\frac{\alpha\mu_0 M_s\Delta\pi^2}{6\gamma_0}\left(\tan^2\chi + \left(\frac{w}{\pi\Delta}\right)^2\frac{1}{\cos^2\chi}\right) = -\sigma\tan\chi + \pi D\cos(\psi - \chi) + \mu_0 H_k M_s\Delta\sin 2(\psi - \chi), \tag{4}$$

where σ is the wall energy per unit area with $\sigma = 4\sqrt{AK} + \pi D\sin(\psi - \chi) + \mu_0 H_k M_s\Delta\sin^2(\psi - \chi) + \pi\Delta M_s H_y\cos\psi$, with H_k the DW demagnetizing field. These equations can be easily generalized to include the effects of the spin transfer torque as well as nonconstant Δ [19,29,30].

Assuming that $\alpha w \gg \Delta$, these equations lead to a typical time scale for the tilting to settle $\tau = \alpha\mu_0 M_s w^2/(6\sigma\gamma_0\Delta)$. The w^2 dependence is explained by the time to reverse the spins in the nanotrack surface swept by the DW when the tilting takes place. On the other hand, the magnetization angle in the DW frame relaxes on a shorter time scale $\tau_\Phi = (1 + \alpha^2)/[\alpha\gamma(\pi D/(2M_s\Delta) - H_k)]$ which does not depend on w. In the steady state regime ($\dot{\chi} = 0$, $\dot{\psi} = 0$) and for $H_y = 0$, the tilt angle is directly related to the DW velocity v as

$$\tan\chi = \frac{2M_s}{\gamma\sigma}v\cos\chi, \tag{5}$$

with the DW velocity $v = (\gamma_0\Delta/\alpha\cos\chi)(H_z + (\pi/2)H_{SO}J\sin\psi)$. This points to the dynamical origin of the DW tilting. Another physical picture can be obtained from the expression of the Lagrangian integrated over the nanotrack $L_{DW}/(t_m w) = \sigma/\cos\chi - 2M_s(\Phi + \chi)\dot{q}/\gamma$, where Φ is the magnetization angle in the DW frame ($\Phi = \psi - \chi$). The first term is the DW internal energy proportional to the DW surface which scales as $1/\cos\chi$. The second term can be seen as a kinetic potential [27], which contrary to a kinetic energy, is linear in the DW velocity and the DW angle. For the field driven case in the steady state regime, Φ is defined only by the in-plane torques due to H_z, D, and H_k [see Eqs. (2) and (3)] and does not depend on χ. The tilt angle in the steady state regime can thus be deduced from the minimization of L_{DW} with χ at fixed Φ, which leads to Eq. (5). Thus the tilt angle is the result of a balance between the gain in the kinetic potential resulting from the DW tilting and the cost in the increased DW energy due to the larger surface.

We now compare the predictions of this model with the results of the micromagnetic simulations. The continuous lines on Figs. 1(c) and 1(d) show the DW tilting induced by H_y predicted by the CCM, whereas the DW tilt angle, time dependence, and DW velocity driven by H_z are plotted in continuous lines on Figs. 2(b)–2(d): a general good agreement is obtained with the micromagnetic simulations despite the simplicity of the model. We also plotted the results of the standard (q, ψ) model on Fig. 2(d) (dashed line). The model does not reproduce the nonlinear increase of the DW velocity, but a good agreement is obtained when considering the DW velocity in the direction perpendicular to its surface v_n (inset). Thus, the DW tilting does not affect DW velocity perpendicular to its surface when driven by H_z.

We now consider the current driven DW dynamics induced by the Slonczewski-like spin-orbit torque in the presence of a large DMI. This torque is expected for samples with SIA such as Pt/Co/AlOx trilayers

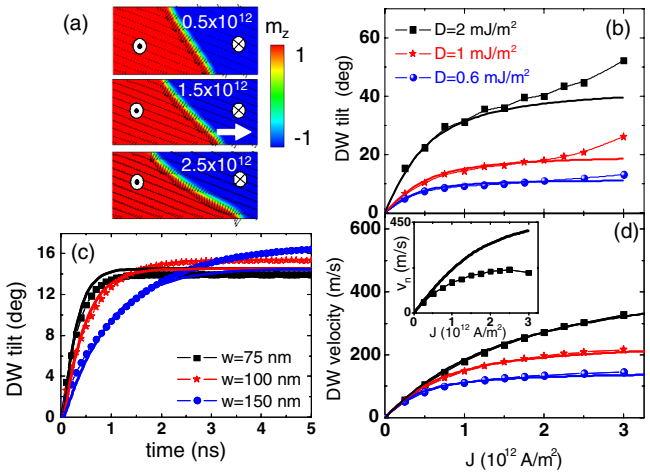

FIG. 3 (color online). Dynamics of the DW driven by the spin-orbit torque [$\mu_0 H_{SO} = 0.1$ T/(10^{12} A/m^2)] for a 100-nm-wide nanotrack. The results of the micromagnetic simulation (CCM) are plotted in colored dots (continuous lines). (a) Magnetization pattern of the DW for $D = 2$ mJ/m^2 and different values of J. The white arrow indicates the current direction. (b),(d) Tilt angle (b) and velocity (d) of the DW as a function of J for different values of D. The inset in (d) shows the DW velocity in the direction perpendicular to the DW surface v_n for $D = 2$ mJ/m^2. The continuous black line is the result of the standard (q, ψ) model. (c) Time dependence of the DW tilt angle for different track widths w for a current of density 0.25×10^{12} A/m^2 applied at $t = 0$ ($D = 2$ mJ/m^2).

[4,8,22]. It may arise from the spin Hall effect due to the current flowing in the nonmagnetic layer and/or from the Rashba spin-orbit interaction [4,6,31]. It leads to an effective easy-axis magnetic field on the DW $H_{SO}J$ proportional to $\sin\psi$ [see Eq. (2)], which thus, is maximal for a Néel DW configuration ($\psi = \pm\pi/2$). The field H_{SO} can be very large $\sim$0.07 T/(10^{12} A/m^2) in Pt/Co/AlOx [21] (see also Refs. [5,15,32,33]). Similar to the action of H_y, the SOT tends to rotate the DW magnetization along the y direction away from the Néel configuration, providing an additional source for the DW tilting.

The results of micromagnetic simulations of the DW dynamics driven by SOT with $\mu_0 H_{SO} = 0.1$ T/(10^{12} A/m^2) are shown in Fig. 3. When injecting a current in the track, a fast DW motion is observed against the electron flow and the velocity increases with J and D [see Fig. 3(d)]. At the same time, a significant tilting of the DW occurs [see Fig. 3(a) for $D = 2$ mJ/m^2], which increases with J and D [Fig. 3(b)]. The DW velocity and the tilting predicted by the CCM are shown on Figs. 3(b) and 3(d), continuous lines. An excellent agreement is obtained with the micromagnetic simulations except at higher current densities for the tilt angle due to the onset of a more complex DW structure [see Fig. 3(a) for $J = 2.5 \times 10^{12}$ A/m^2]. The DW velocity in the direction perpendicular to the DW surface v_n for $D = 2$ mJ/m^2 is plotted on Fig. 3(d), inset. Contrary to the field driven case, the standard (q, ψ) model strongly overestimates the DW velocity (continuous line). The DW tilting leads to an additional rotation of the DW angle ψ away from $\pi/2$ where the torque is maximal. Thus, the DW tilting leads to a large decrease of the DW velocity. This clearly illustrates the importance of the DW tilting on the CIDM for large DMIs. Figure 3(c) shows the time dependence of the tilting for a current step of $J = 0.25 \times 10^{12}$ A/m^2 applied at $t = 0$. The CCM (continuous lines) reproduces well the time scale for the tilting to take place which scales as w^2.

Experimentally, Ryu *et al.* recently reported fast current induced DW motion associated with a significant DW tilting in perpendicularly magnetized (Pt/Co/Ni/Co/TaN) nanotracks with SIA [14,20]. By studying the dependence of the current induced DW velocity on an in-plane longitudinal magnetic field, they present evidence of chiral DWs driven by the Slonczewski-like SOT in agreement with the presence of DMI. The DW tilting is reversed for up (down) and down (up) DW which is well explained by Néel DWs pointing in opposite directions due to the DMI. From the longitudinal magnetic field required to suppress the CIDM and using the magnetic and transport parameters of Ref. [14,20], one can deduce a DMI of $D = 0.8$ mJ/m^2 for $A = 1 \times 10^{-11}$ J/m. Using this value, micromagnetic simulations predict a steady state tilt angle of about 18° for $J = 1 \times 10^{12}$ A/m^2 close to the one measured experimentally ($\sim$20°) [19]. Note that smaller additional contributions may arise from the anomalous Hall effect and the Oersted field [19], and DW pinning may also affect the results. Thus, our model accounts for the DW tilting reported by Ryu *et al.*

To conclude, we have shown that the DMI can lead to a large tilting of the DW surface in perpendicularly magnetized nanotracks when DW dynamics are driven by an easy axis magnetic field or a spin polarized current. The DW tilting strongly affects the DW dynamics for large DMI, and the tilting relaxation time can be very large as it scales with the square of the track width. We propose a simple way to estimate the DMI in magnetic multilayers by measuring the dependence of the DW tilt angle on a transverse static magnetic field. Our results propose an explanation for the current-induced DW tilting observed in perpendicularly magnetized Co/Ni multilayers with SIA [20] where chiral effects were reported [14] and are in agreement with the DMI scenario in these samples.

This work was supported by project Agence Nationale de la Recherche, Project No. ANR 11 BS10 008 ESPERADO.

*olivier.boulle@cea.fr

[1] I. E. Dzyaloshinskii, Sov. Phys. JETP **5**, 1259 (1957).
[2] T. Moriya, Phys. Rev. **120**, 91 (1960).
[3] M. Bode, M. Heide, K. von Bergmann, P. Ferriani, S. Heinze, G. Bihlmayer, A. Kubetzka, O. Pietzsch,

S. Blügel, and R. Wiesendanger, Nature (London) **447**, 190 (2007).
[4] I. M. Miron, K. Garello, G. Gaudin, P.-J. Zermatten, M. V. Costache, S. Auffret, S. Bandiera, B. Rodmacq, A. Schuhl, and P. Gambardella, Nature (London) **476**, 189 (2011).
[5] L. Liu, O. J. Lee, T. J. Gudmundsen, D. C. Ralph, and R. A. Buhrman, Phys. Rev. Lett. **109**, 096602 (2012).
[6] L. Liu, C.-F. Pai, Y. Li, H. W. Tseng, D. C. Ralph, and R. A. Buhrman, Science **336**, 555 (2012).
[7] I. M. Miron, P.-J. Zermatten, G. Gaudin, S. Auffret, B. Rodmacq, and A. Schuhl, Phys. Rev. Lett. **102**, 137202 (2009).
[8] I. M. Miron *et al.*, Nat. Mater. **10**, 419 (2011).
[9] A. Thiaville, S. Rohart, E. Jué, V. Cros, and A. Fert, Europhys. Lett. **100**, 57 002 (2012).
[10] M. Heide, G. Bihlmayer, and S. Blügel, Phys. Rev. B **78**, 140403((2008).
[11] G. Chen *et al.*, Phys. Rev. Lett. **110**, 177204 (2013).
[12] A. V. Khvalkovskiy, V. Cros, D. Apalkov, V. Nikitin, M. Krounbi, K. A. Zvezdin, A. Anane, J. Grollier, and A. Fert, Phys. Rev. B **87**, 020402 (2013).
[13] P. P. J. Haazen, E. Murè, J. H. Franken, R. Lavrijsen, H. J. M. Swagten, and B. Koopmans, Nat. Mater. **12**, 299 (2013).
[14] K. Ryu, L. Thomas, S. Yang, and S. Parkin, Nat. Nanotechnol. **8**, 527 (2013).
[15] S. Emori, U. Bauer, S.-M. Ahn, E. Martinez, and G. S. D. Beach, Nat. Mater. **12**, 611 (2013).
[16] D. Partin, M. Karnezos, L. deMenezes, and L. Berger, J. Appl. Phys. **45**, 1852 (1974).
[17] M. Viret, A. Vanhaverbeke, F. Ott, and J.-F. Jacquinot, Phys. Rev. B **72**, 140403 (2005).
[18] M. Yamanouchi, D. Chiba, F. Matsukura, T. Dietl, and H. Ohno, Phys. Rev. Lett. **96**, 096601 (2006).
[19] See Supplemental Material at http://link.aps.org/supplemental/10.1103/PhysRevLett.111.217203 for a discussion on other mechanisms which can lead to DW tilting, as well as the effect of the spin transfer torque and field like SOT on the DW tilting.
[20] K.-S. Ryu, L. Thomas, S.-H. Yang, and S. S. P. Parkin, Appl. Phys. Express **5**, 093006 (2012).
[21] K. Garello, I. M. Miron, C. O. Avci, F. Freimuth, Y. Mokrousov, S. Blügel, S. Auffret, O. Boulle, G. Gaudin, and P. Gambardella, Nat. Nanotechnol. **8**, 587 (2013).
[22] I. M. Miron, G. Gaudin, S. Auffret, B. Rodmacq, A. Schuhl, S. Pizzini, J. Vogel, and P. Gambardella, Nat. Mater. **9**, 230 (2010).
[23] H. Szambolics, J. C. Toussaint, A. Marty, I. M. Miron, and L. D. Buda-Prejbeanu, J. Magn. Magn. Mater. **321**, 1912 (2009).
[24] S. Rohart and A. Thiaville, arXiv:1310.0666v1.
[25] See also the corresponding movie for $w = 100$ nm in the Supplemental Material [19].
[26] A. Malozemoff and J. Slonczewski, *Magnetic Domain Walls in Bubble Materials* (Academic Press, New York, 1979).
[27] A. Hubert, *Theorie der Domänenwände in Geordneten Medien* (Springer, Berlin, 1974).
[28] A. Thiaville, J. M. Garcia, and J. Miltat, J. Magn. Magn. Mater. **242–245**, 1061 (2002).
[29] O. Boulle, L. D. Buda-Prejbeanu, M. Miron, and G. Gaudin, J. Appl. Phys. **112**, 053901 (2012).
[30] A. Thiaville, Y. Nakatani, J. Miltat, and Y. Suzuki, Europhys. Lett. **69**, 990 (2005).
[31] P. M. Haney, H. W. Lee, K. J. Lee, A. Manchon, and M. D. Stiles, Phys. Rev. B **87**, 174411 (2013).
[32] U. H. Pi, K. W. Kim, J. Y. Bae, S. C. Lee, Y. J. Cho, K. S. Kim, and S. Seo, Appl. Phys. Lett. **97**, 162507 (2010).
[33] J. Kim, J. Sinha, M. Hayashi, M. Yamanouchi, S. Fukami, T. Suzuki, S. Mitani, and H. Ohno, Nat. Mater. **12**, 240 (2012).